

Application of a Commercial Lidar-Ceilometer to Studies of Aerosols in the Atmospheric Boundary Layer

Arshath Ramkilowan^{a,*} and Derek J. Griffith^a

^aCSIR Defence, Peace Safety and Security

Optronics Sensor Systems, Pretoria, South Africa.

*Corresponding author. Email: aramkilowan@csir.co.za. Tel: +27 12 841 4859

Abstract

Ceilometers operating on several optical principles have been extensively applied to vertical visibility and cloud base measurements relating to aviation safety. The latest generation of laser time-of-flight backscatter ceilometers use the same optical sounding principle as more powerful and costly research lidar systems. Ceilometers in persistent and unattended operation have become ubiquitous for aviation safety, particularly in Europe and the USA and their potential for use in aerosol studies has therefore become of great interest. CSIR/DPSS has acquired and deployed a Vaisala CL51 ceilometer chiefly for the purpose of investigating the vertical distribution of aerosols in the Atmospheric Boundary Layer (ABL) and cloud base height for application in the modelling of optical surveillance through the ABL. We show some results from ABL analysis of CL51 backscatter data and explore the potential for retrieval of more quantitative aerosol properties such as the lidar ratio. The latter retrievals can be either compared to or calibrated using complementary measurements such as those from AERONET sun-photometers. We conclude that commercial lidar/ceilometers such as the Vaisala CL51 offer cost-effective and long-term potential for aerosol studies in the optical surveillance and atmospheric radiative transfer applications.

Keywords: Lidar, ceilometer, aerosol studies, atmospheric boundary layer

1. Introduction

Backscatter lidar systems are powerful remote-sensing tools for investigation of the structure and composition of the atmosphere. Research-grade lidars are high cost systems that are typically only operated in a supervised mode. Compact, robust, eye-safe and cost-effective laser ceilometers operating on the lidar principle have become an essential tool in aviation safety. While less capable than research lidars, the widespread and long-term deployment [1] of such ceilometers in unsupervised operation has led to strong interest in the application of these instruments to atmospheric research [2,3,4,5]. This is particularly the case in relation to the spatial distribution, transport and optical properties of aerosol particles in the atmospheric boundary layer (ABL).

CSIR/DPSS has been operating a Vaisala CL51 lidar-ceilometer since late 2014 in order to investigate applicability to establishing a local climatology for the vertical distribution of aerosols and clouds. In our case, such a climatology is important for statistical modelling of the effectiveness of optical surveillance systems viewing targets through the ABL, particularly from airborne platforms.

Potential application of lidar-ceilometer systems could also be found in ABL studies for climate, meteorology and air quality.

2. Instrumentation

The Vaisala CL51 is a commercial lidar ceilometer that measures laser backscatter at a wavelength of 910 nm as a function of height above ground up to a maximum height of 15 km and with a range resolution of 10 m. The optical design is monostatic, meaning that the same optical

aperture is used for laser transmission and detection. The monostatic design has full optical overlap to ground level, which is a useful feature for aerosol studies.

The instrument is primarily stationed in a peri-urban environment atop a building at the CSIR, Pretoria campus (25.757°S, 27.280°E) 25 m above ground level at an altitude of 1449 m. Data from a temporary installation of the instrument in Simon's Town is also considered. This setup, also on the roof of a building is 22 m above ground level, 25 m above sea level and in a coastal environment.

Other instrumentation used in this study includes the Cimel CE318 robotic sun-photometer, which is the standard instrument used in the AEROSOL ROBOTIC NETWORK (AERONET) [6] for measurement of Aerosol Optical Depth (AOD) and other aerosol optical properties.

3. Theory and Methods

The elastically backscattered optical power P received by a lidar system from a vertical range (height) z can be expressed as [7]

$$P(z) = C_L \frac{\beta(z)}{z^2} \exp\{-2 \int_0^z \alpha(z') dz'\},$$

where $\beta(z)$ is the volume backscatter coefficient as a function of height, $\alpha(z)$ is the extinction (attenuation) coefficient and C_L is a lidar system calibration constant. The backscatter and extinction coefficients can be separated into that from aerosol particles and that from molecules. In the near-infrared (910 nm wavelength in the case of the CL51), the backscatter due to molecules will be neglected and is usually below the noise floor in the case of low-power ceilometers. It is further assumed that the received signal is

single-scattered (not valid at high optical depth, such as in clouds).

The Vaisala CL51 reports the two-way attenuated backscatter profile [8]

$$\beta'(z) = \beta(z) \exp\{-2 \int_0^z \alpha(z') dz'\} = \frac{P(z)z^2}{c_L}$$

This means that the instrument constant has been determined by the manufacturer. There is currently little information available on the accuracy and stability of the instrument constant so we assume reliability and cannot yet perform a credible uncertainty analysis.

The backscatter and extinction coefficients are related through the lidar ratio S_p as

$$\alpha(z) = S_p(z)\beta(z).$$

The lidar ratio is often assumed constant with height in aerosol layers and then written simply as S_p .

The argument of the exponential function above is twice the optical depth $\tau(z)$ from ground level to height z i.e.

$$\beta'(z) = \beta(z)e^{-2\tau(z)}$$

The differential increase in optical depth at height z can be expressed as

$$d\tau = \alpha(z)dz = S_p(z)\beta(z)dz.$$

Following the calibration argument presented by Vande Hey [7], integrating the attenuated backscatter profile over the full atmospheric column yields

$$B = \int_0^\infty \beta'(z)dz = \int_0^\infty \beta(z)e^{-2\tau(z)}dz.$$

Assuming the lidar ratio constant with height in a cloudless scenario and changing the integration variable to τ provides

$$B = \frac{1}{S_p} \int_0^{\tau_{top}} e^{-2\tau} d\tau = \frac{1 - e^{-2\tau_{top}}}{2S_p},$$

where τ_{top} is the full vertical aerosol optical depth from ground to top-of-atmosphere. If τ_{top} is available from a sun-photometer measurement, it is possible to estimate the height-independent lidar ratio from the CL51 output profile as

$$S_p = \frac{1 - e^{-2\tau_{top}}}{2B}.$$

The total vertical aerosol optical depth (AOD) at 910 nm can be interpolated from data reported by the AERONET sun-photometer which is located at DPSS in close proximity to the ceilometer.

Conversely, if a reasonable estimate of the lidar ratio is available it is possible to estimate the vertical AOD from the ceilometer profile as

$$\tau_{top} = \frac{-\ln(1 - 2BS_p)}{2}$$

The latter approximation is potentially useful in our work to estimate the AOD at night using CL51 backscatter data when the sun-photometer is inoperable.

If the extinction coefficient α can be considered uniform in the aerosol layer, the simple model for $\tau(z)$ up to the top of the layer z_{top} is

$$\tau(z) = \alpha z,$$

so that

$$\tau_{top} = \alpha z_{top}$$

and

$$\alpha = \frac{-\ln(1 - 2B_{top}S_p)}{2z_{top}}.$$

This last expression is potentially useful in our optical surveillance application for providing an estimate of the aerosol extinction coefficient at 910 nm using a reasonable estimate of the lidar ratio when dealing with a cloudy scenario by performing integration of the ceilometer backscatter profile up to the first cloud base. It can also form the basis of estimating horizontal visibility near the surface by integrating only over the first few height bins. For example, visibility (surface meteorological range) in km is computed in the MODTRAN[®] radiative transfer code using [9]

$$VIS = \frac{\ln(50)}{\alpha_{550} + 0.01159},$$

where α_{550} is the extinction coefficient at 550 nm in units of km^{-1} .

4. Results and discussion

Four clear days have been selected for computation of the lidar ratio according to the above procedure.

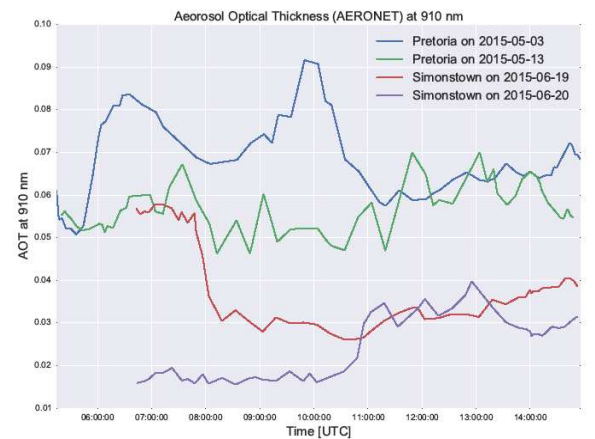


Figure 1: Aerosol Optical Depth from AERONET Cimel CE318 sun-photometers at CSIR/Pretoria and IMT/Simon's Town.

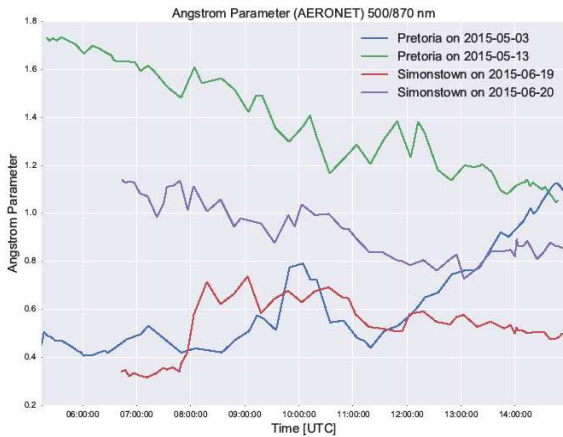


Figure 2 Angstrom parameter from AERONET Cimel CE318 sun-photometers at CSIR/Pretoria and IMT/Simon's Town

Two days were taken from the ceilometer operational period in Pretoria and another two days from the period in Simon's Town.

The four days in question were chosen in order to cover both inland and maritime aerosol characters, as well as a variety of AOD and Angstrom parameter values.

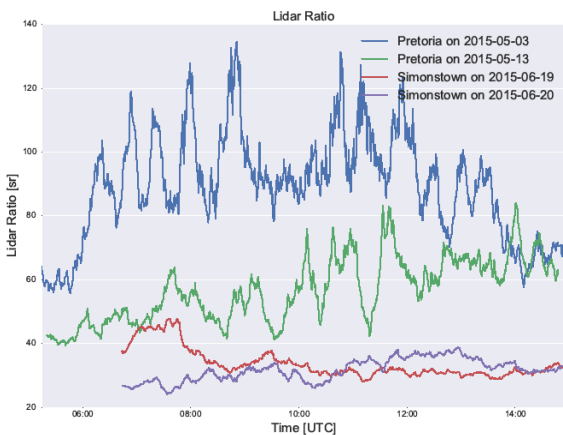


Figure 3: Lidar Ratios computed from ceilometer backscatter profiles in conjunction with AERONET sun-photometer AOD.

Figure 1 provides the AOD from AERONET for all four days, while the Angstrom parameter (spanning wavelengths 500 nm to 870 nm) is shown in Figure 2. Higher Angstrom parameter and lower lidar ratio are both generally associated with smaller particle size and would therefore be expected to show an inverse correlation. For example, 2015-05-13 at Pretoria shows relatively constant AOD, but declining Angstrom parameter, whereas the lidar ratio is clearly increasing in inverse correlation with the Angstrom parameter.

The magnitudes of the computed lidar ratios are generally plausible, but the strong variations at the Pretoria station do

require explanation. Current reasoning attributes such variations partially to the difference in temporal sampling, 15 s for the ceilometer compared to the ± 15 minute sampling resolution of the AERONET node. Additionally, the CL51 samples an air mass volume extending 15 km directly upwards from the instrument whereas the sun-photometer collects data integrated along the node-sun path.

Computation of the lidar ratio from a combination of ceilometer and sun-photometer data makes numerous assumptions and approximations and the uncertainty is impossible to quantify without an independent calibration of the CL51. A further factor which has been neglected is that the operating wavelength of the CL51 (910 nm) lies just within the wing of a water-vapour absorption band. The backscatter profile is therefore impacted by the water vapour vertical profile and total column. Corrections for this are potentially required depending on the level of accuracy that is needed. Wiegner and Gasteiger [10] provide a methodology for correcting ceilometer data for water vapour absorption in such instances. The rapid fluctuations of the ceilometer backscatter profiles are thought to be a manifestation of uncharacterised hygroscopic growth of the aerosol particles as well as particle quantity. An investigation of humidity and wind profiles is required to confirm this hypothesis.

5. Boundary Layer Analysis

Vaisala offers a software package for boundary layer analysis called BL-VIEW [11]. This package uses a negative gradient algorithm with vertical and temporal averaging procedures on backscatter profiles passed through cloud and precipitation filters to identify candidate heights for the tops of aerosol layers and cloud bases. BL-VIEW is set up by default to report up to 3 candidate aerosol ceilings and up to 3 cloud base candidates. This data can be used, for instance, to gather statistics on diurnal and seasonal variation in ABL height.

5.1 Diurnal ABL Height

Typical results from BL-VIEW for a cloudless day in which the height of the ABL (broadly identified with the mixing layer for air quality purposes) is strongly driven by convection are shown in Figure 4.

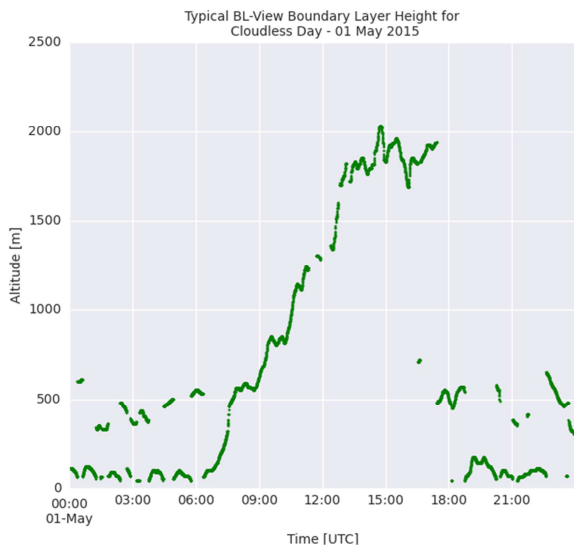


Figure 4: Boundary layer height candidates identified by BL-VIEW at Pretoria on 2015-05-01

5.2 Seasonal ABL Height

A seasonal trend in ABL height is also to be expected. For days meeting a low-cloud criterion of 80% (meaning that 80% of BL-VIEW measurements detected no cloud base), the first BL-VIEW height candidate for the ABL ceiling has been aggregated for the period around local noon, over the 8 months for which the CL51 was operational in Pretoria. The results are shown in Figure 5.

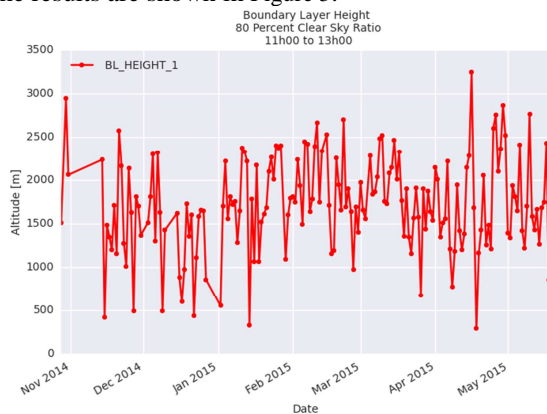


Figure 5: Daily mean ABL height candidates from BL-VIEW on days with less than 20% ceilometer cloud hits at Pretoria

Figure 5 clearly shows how the convective boundary layer becomes more compact in winter. For all data, including all data with cloud hits, this seasonal trend is partially masked by high prevalence of low level cloud hits in summer. This is seen in Figure 6.

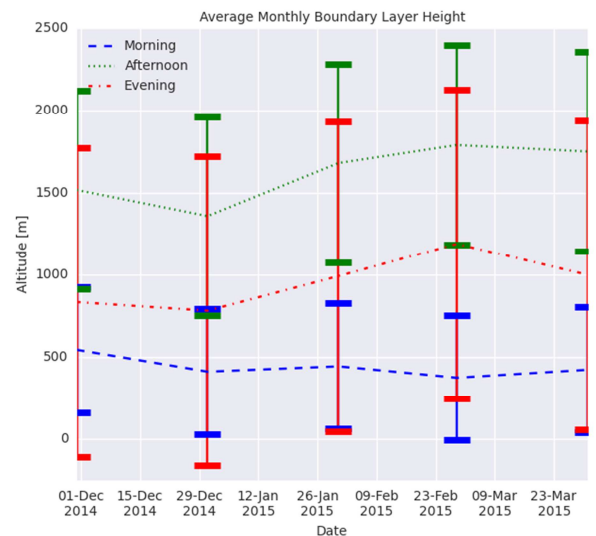


Figure 6: Monthly averages of all BL-VIEW ABL height candidates, including measurements with cloud hits (Pretoria site).

6. Conclusions

In general, lidar-ceilometers do not have sufficient laser power to allow absolute calibration from Rayleigh backscatter in clear air (free troposphere) which is a common calibration method for higher power research lidars. In the absence of additional data, this restricts the use of such ceilometers to determination of ABL and cloud base height with less reliable quantitative determination of the vertical distribution or optical properties. With a total aerosol optical depth obtained from a sun-photometer (e.g. AERONET), it becomes possible to estimate the lidar ratio and conversely, with a reasonable estimate of the lidar ratio it becomes possible to estimate total AOD and the extinction coefficient in simple situations.

The data yielded by the CL51 in conjunction with AERONET data will provide climatologies for ABL height and cloud base to be used in statistical models of optical surveillance system effectiveness. Extrapolations of aerosol optical depth and optical extinction to cloudy scenarios and night scenarios will be possible but with increased uncertainty. Methods for independent calibration (e.g. Jin [12]) and uncertainty assessment will have to be adopted or developed.

7. References

- [1] Deutscher Wetterdienst (2015), 'DWD Ceilometer Viewer', DWD, <http://www.dwd.de/ceilomap>. Accessed 2015-07-20.
- [2] Flentje, H.; Heese, B.; Reichardt, J. & Thomas, W. (2010), 'Aerosol profiling using the ceilometer network of the German Meteorological Service', Atmospheric Measurement Techniques Discussions 3(4), 3643--3673.
- [3] Jin, Y.; Kai, K.; Kawai, K.; Nagai, T.; Sakai, T.; Yamazaki, A.; Uchiyama, A.; Batdorj, D.; Sugimoto, N. & Nishizawa, T. (2015), 'Ceilometer calibration for retrieval

of aerosol optical properties ', *Journal of Quantitative Spectroscopy and Radiative Transfer* 153, 49 - 56.

[4] Wiegner, M.; Madonna, F.; Biniotoglou, I.; Forkel, R.; Gasteiger, J.; Geiß, A.; Pappalardo, G.; Schädler, K. & Thomas, W. (2014), 'What is the benefit of ceilometers for aerosol remote sensing? An answer from EARLINET', *Atmospheric Measurement Techniques* 7(7), 1979--1997.

[5] Wiegner, M. & Geiß, A. (2012), 'Aerosol profiling with the Jenoptik ceilometer CHM15kx', *Atmospheric Measurement Techniques* 5(8), 1953--1964.

[6] NASA Goddard Space Flight Center (2015), 'The AEROSOL ROBOTIC NETWORK (AERONET)', National Aeronautics and Space Administration (USA), <http://aeronet.gsfc.nasa.gov/>. Accessed 2015-07-20.

[7] Vande Hey, J. (2014), *A Novel Lidar Ceilometer: Design, Implementation and Characterisation*, Springer International Publishing.

[8] Vaisala Oyj (2010), 'User's Guide : Vaisala Ceilometer CL51', <http://www.vaisala.com>.

[9] Berk, A.; Anderson, G.; Acharya, P. & Shettle, E. (2008), 'MODTRAN 5.2.0.0 User's Manual', Spectral Sciences, Inc. and Air Force Research Laboratory (AFRL), <http://www.modtran5.com/>.

[10] Wiegner, M. & Gasteiger, J. (2015), 'Correction of water vapor absorption for aerosol remote sensing with ceilometers', *Atmospheric Measurement Techniques Discussions* 8(6), 6395--6438.

[11] Vaisala Oyj (2010), 'User's Guide : Vaisala Boundary Layer View Software BL-VIEW', <http://www.vaisala.com>.

[12] Jin, Y.; Kai, K.; Kawai, K.; Nagai, T.; Sakai, T.; Yamazaki, A.; Uchiyama, A.; Batdorj, D.; Sugimoto, N. & Nishizawa, T. (2015), 'Ceilometer calibration for retrieval of aerosol optical properties ', *Journal of Quantitative Spectroscopy and Radiative Transfer* 153, 49 - 56.